Geobiology

Geobiology (2013), **11**, 307–317 DOI: 10.1111/gbi.12038

Global deglaciation and the re-appearance of microbial matground-dominated ecosystems in the late Paleozoic of Gondwana

L. A. BUATOIS,[1] R. G. NETTO,[2] M. GABRIELA MÁNGANO[1] AND N. B. CARMONA[1,*]

[1]*Department of Geological Sciences, University of Saskatchewan, Saskatchewan, SK, Canada*
[2]*PPGeo UNISINOS, São Leopoldo RS, Brazil*

ABSTRACT

The extensive matgrounds in Carboniferous-Permian open-marine deposits of western Argentina constitute an anachronistic facies, because with the onset of penetrative bioturbation during the early Paleozoic microbial mats essentially disappeared from these settings. Abundant microbially induced sedimentary structures in the Argentinean deposits are coincident with the disappearance of trace and body fossils in the succession and with a landward facies shift indicative of transgressive conditions. Deposits of the Late Carboniferous–Early Permian glacial event are well developed in adjacent basins in eastern Argentina, Brazil, South Africa and Antarctica, but do not occur in the western Andean basins of Argentina. However, the deglaciation phase is indirectly recorded in the studied region by a rapid rise in sea level referred to as the Stephanian-Asselian transgression. We suggest that an unusual release of meltwater during the final deglaciation episode of the Gondwana Ice Age may have dramatically freshened peri-Gondwanan seas, impacting negatively on coastal and shallow-marine benthic faunas. Suppression of bioturbation was therefore conducive to a brief re-appearance of matground-dominated ecosystems, reminiscent of those in the precambrian. Bioturbation is essential for ecosystem performance and plays a major role in ocean and sediment geochemistry. Accordingly, the decimation of the mixed layer during deglaciation in the Gondwana basins may have altered ecosystem functioning and geochemical cycling.

Received 17 November 2012; accepted 26 March 2013

Corresponding author: L. A. Buatois. Tel.: 1 306 966 5730; fax: 1 306 966 8593; e-mail: luis.buatois@usask.ca

*Present address: CONICET-UNRN, Instituto de Investigación en Paleobiología y Geología, Universidad Nacional de Río Negro, Isidro Lobo y Belgrano, Río Negro, Argentina

INTRODUCTION

Ediacaran marine ecosystems were dominated by extensive matgrounds and, as a result, deposits are characterized by a suite of microbially induced sedimentary structures (MISS of Noffke *et al.*, 2001), such as wrinkle marks, ripple patches and palimpsest ripples (Seilacher & Pflüger, 1994; Seilacher, 1999; Noffke, 2010). Infaunalization and the concomitant appearance of vertical bioturbation during the Cambrian agronomic revolution resulted in the restriction of matgrounds to inhospitable environments, such as hypersaline lagoons and anoxic settings (Seilacher & Pflüger, 1994; Hagadorn & Bottjer, 1999; Seilacher, 1999; Pflüger, 1999; Buatois & Mángano, 2011a,b). However, matgrounds reappeared in shallow-marine environments as a result of global biotic crises, as indicated by the end-Permian mass extinction (Pruss *et al.*, 2004; Mata & Bottjer, 2012; Ezaki *et al.*, 2012).

The late Paleozoic Gondwanan glaciation and its subsequent deglaciation phase undoubtedly exerted a global impact on marine ecosystems, as indicated by the low levels of rates of origination and extinction of marine organisms during the glacial events (Stanley & Powell, 2003), and the substantial changes in the composition of marine communities in postglacial times (Clapham & James, 2008). In addition, deglaciation resulted in direct local impact on coastal communities due to the strong meltwater discharge issuing from melting of the continental ice masses (Buatois *et al.*, 2006, 2010). Although global and local effects of the Gondwana glaciation have been explored, its impact at regional scale is not well understood. The aim of this paper

is to: (i) document an anachronistic occurrence of widespread matgrounds in Carboniferous–Permian shallow-marine deposits of western Argentina, and (ii) evaluate how the re-appearance of matground-dominated ecosystems should be understood within the framework of the deglaciation phase in Gondwana, underscoring the geobiological impact of meltwater discharge.

STRATIGRAPHY AND AGE

The Carboniferous–Permian back–arc Calingasta–Uspallata Basin of western Argentina (Fig. 1) is part of a series of perigondwanic basins developed along the paleo-Pacific margin (López-Gamundí, 2010). The Santa Elena Formation is exposed in Sierra de Uspallata, forming the southernmost outcrops of this basin (Dessanti & Rossi, 1950). It has been subdivided into the Tramojo and Jarillal members, the former encompassing mostly continental deposits and the latter being marine in origin (Taboada, 1998, 1999). Based on the presence of brachiopods of the *Tivertonia–Streptorhynchus* and *Cancrinella* (= *Costatumulus*) biozones, the Jarillal Member is considered of Stephanian-Asselian age (Taboada, 1998, 1999; Azcuy *et al.*, 1999).

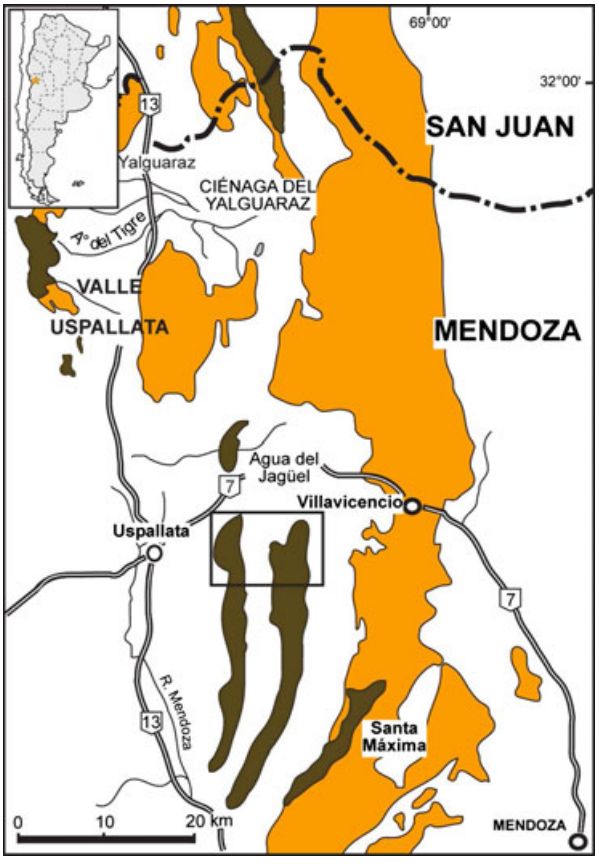

Fig. 1 Geological map showing distribution of upper Paleozoic outcrops in the Calingasta-Uspallata Basin (after Azcuy *et al.*, 1999). Box indicates location of study area.

SEDIMENTARY FACIES AND DEPOSITIONAL ENVIRONMENTS

The Jarillal Member in Sierra de Uspallata has been subdivided into three main intervals (Fig. 2). Two facies associations: A (Wave-dominated shallow marine) and B (Mixed wave- and river-influenced delta) have been recognized (Table 1). The

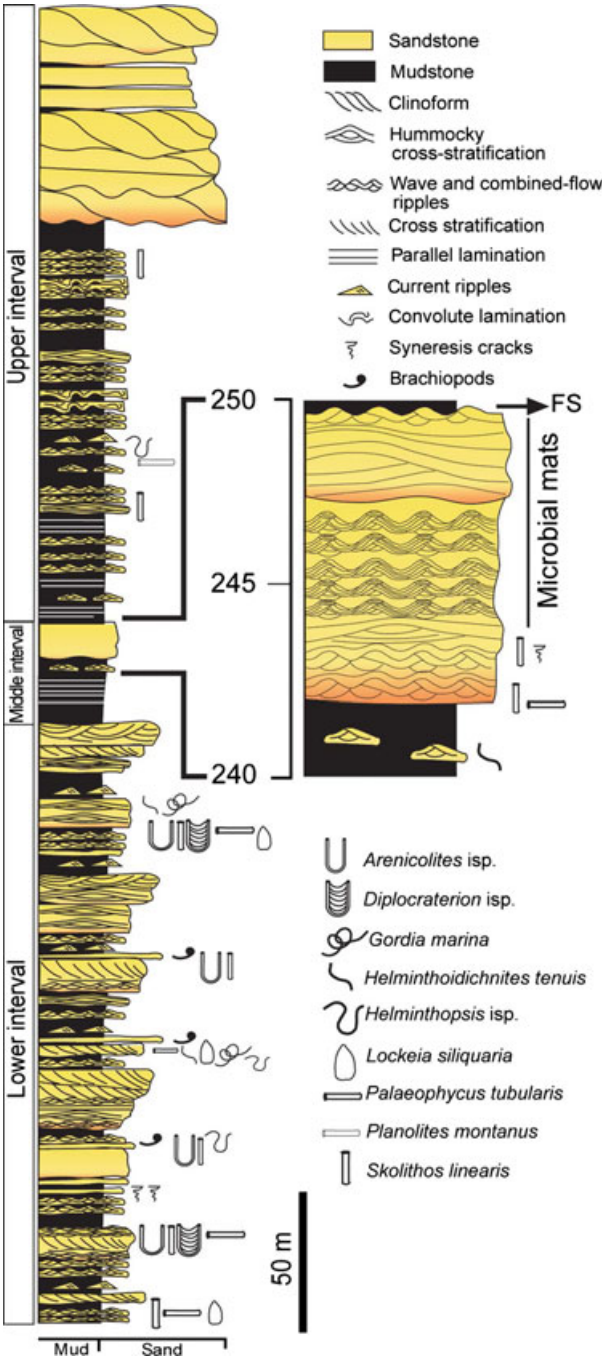

Fig. 2 Sedimentologic log of the Jarillal Member of the Santa Elena Formation in Sierra de Uspallata, showing a detailed view of the interval containing the matground facies at the top of a wave-dominated parasequence.

Table 1 Sedimentary facies of the Jarillal Member, Santa Elena Formation, Sierra de Uspallata, western Argentina. MISS occur in lower/middle-shoreface deposits (Facies A5).

Facies associations	Facies	Lithology & sedimentary structures	Trace fossils	Sedimentary processes	Sedimentary environment
Facies Association A: Wave-dominated shallow marine	Facies A1: Parallel-laminated and massive mudstone	Parallel-laminated or massive dark grey mudstone forming laterally persistent intervals up to 30 m thick	None	Suspension fall-out under low-energy conditions below the storm wave base	Shelf
	Facies A2: Siltstone with thinly bedded very fine-grained sandstone	Massive or parallel-laminated, tabular, dark grey, siltstone units intercalated with sharp-based, tabular or lenticular sandstone beds. Sandstone is 0.1–5 cm thick and siltstone is 20–350 cm thick. Beds are stacked forming intervals up to 14.60 m thick. Thinly bedded very fine-grained sandstone shows parallel lamination, combined-flow ripple cross-lamination and symmetrical to quasi-symmetrical ripple tops. Some sandstone bases contain load casts. Wavy and lenticular bedding present locally. Syneresis cracks are very rare	*Arenicolites* isp., *Gordia marina*, *Helminthoidichnites tenuis*, *Helminthopsis* isp., *Palaeophycus tubularis*, *Skolithos linearis*	Low-energy, suspension fall–out deposition during fair-weather times punctuated by rare, distal storm events. Subordinate tidal influence. Immediately above storm wave base	Lower offshore
	Facies A3: Interbedded wave-rippled fine- to very fine-grained sandstone and siltstone	Massive or parallel-laminated siltstone with, tabular or lenticular, erosive-based, light yellowish grey, fine- to very fine–grained sandstone beds. Sandstone is 3–17 cm thick and siltstone is 4-74 cm thick. Beds are stacked forming intervals up to 7.8 m thick. Sandstone beds show combined-flow and wave ripple-cross and parallel lamination. Mudstone drapes are present locally. Wave length and amplitude increase upward in individual bedsets. Brachiopod concentrations occur in some layers	*Arenicolites* isp., *Diplocraterion parallelum*, *Lockeia siliquaria*, *Palaeophycus tubularis*, *Skolithos linearis*	Alternating background suspension fall-out during fair-weather times and relatively distal storm deposition. Subordinate tidal influence. Closer proximity to the fair-weather wave base	Upper offshore
	Facies A4: Interbedded hummocky cross-stratified very fine- to fine-grained sandstone and siltstone	Intercalations of erosive-based, tabular hummocky cross-stratified fine- to very fine-grained sandstone and parallel-laminated siltstone. Sandstone beds typically form discrete layers rather than amalgamated units. Sandstone is 10–70 cm thick and siltstone is 1–5 cm thick. Beds are stacked forming intervals up to 2.5 m thick. Hummocky beds may pass upwards into a zone with combined-flow ripple cross-lamination and/or symmetrical to quasi-symmetrical ripples and micro-hummocky cross-stratification. Hummocky cross-stratification includes both isotropic and anisotropic types. Abundant mica flakes occur on third-order surfaces of the hummocky and micro-hummocky beds	*Arenicolites* isp., *Gordia marina*, *Helminthopsis* isp., *Skolithos linearis*	Alternation of sediment fall-out during fair-weather times and high-intensity oscillatory flows during frequent storms right below fair-weather wave base	Offshore transition
	Facies A5: Amalgamated hummocky cross-stratified very fine- to fine-grained sandstone	Hummocky cross-stratified, light grey very fine- to fine-grained sandstone forming amalgamated units up to 3.20 m thick. Internal second-order erosion surfaces separating hummocky cross-stratified laminasets are commonly mantled by mudstone intraclasts. Abundant mica flakes occur on third-order surfaces. Bedsets laterally persistent, but individual hummocky beds may pinch out or grade into ripple cross-laminated units. Hummocky cross-stratification includes both isotropic and anisotropic types. Parallel-stratified to low-angle cross-stratified medium- to coarse-grained sandstone beds are present locally, as well as fine- to very fine-grained sandstone with micro-hummocky cross-stratification and wave-ripple cross-lamination. Matground structures occur in this facies at the top of the middle interval	*Arenicolites* isp., *Diplocraterion parallelum*, *Gordia marina*, *Helminthoid-ichnites tenuis*, *Lockeia siliquaria*, *Palaeophycus tubularis*, *Skolithos linearis*	Repeated storm wave activity and wave–generated surges above fair-weather wave base	Lower/middle shoreface
	Facies A6: Trough to planar cross-bedded medium- to very coarse-grained sandstone	Trough to planar cross-bedded, erosive-based, fine- to coarse-grained sandstone forming sets up to 6.30 m thick. Laterally extensive units, although individual beds may show lateral thickness variations, in places displaying lenticular geometries. Erosive surfaces are locally mantled by pebbles and mudstone intraclasts. Dune and current-ripple bedforms are preserved at the top of some layers. Interference ripples locally present. Brachiopod concentrations occur in some layers	*Skolithos linearis*	Multidirectional, strongly erosional, current flows leading to migration of 3D and 2D dunes in the build-up and surf zones.	Upper shoreface channels and bars

Table 1 (continued)

Facies associations	Facies	Lithology & sedimentary structures	Trace fossils	Sedimentary processes	Sedimentary environment
Facies Association B: Mixed wave-and river-influenced delta	Facies B1: Interbedded mudstone, graded siltstone and hummocky cross-stratified and wave-rippled very fine-grained sandstone	Massive or parallel-laminated, tabular, dark grey to black, mudstone intercalated with tabular sharp-based, normally graded to parallel-laminated siltstone and tabular or lenticular, sharp-based, very fine-grained sandstone with wave-ripple cross-lamination, micro-hummocky cross-stratification or hummocky cross-stratification. Mudstone intervals are 1-60 cm thick, siltstone beds are 3-15 cm thick, and sandstone beds are 0.5–45 cm thick. Beds are stacked forming intervals up to 42 m thick. Tool marks are common on sandstone soles. Hummocky cross-stratification includes both isotropic and anisotropic types. Some sandstone beds internally display current-ripple cross-lamination and wave-rippled tops. Climbing-ripple cross-lamination occurs locally. A wide variety of soft-sediment deformation structures, such as load casts, pseudonodules, balls-and-pillows and convolute lamination, occur in the sandstone beds. Siltstone layers may contain starved current ripples. Marl lenses are present locally	*Helminthopsis* isp., *Planolites montanus*	Low-energy, suspension fall–out deposition punctuated by hyperpycnal flows and episodic turbidity currents, affected by wave reworking. Between storm and fairweather wave base	Prodelta of a mixed wave- and river-influenced delta
	Facies B2: Amalgamated hummocky cross-stratified and climbing-ripple cross-laminated, very fine- to fine-grained sandstone	Hummocky cross-stratified to climbing-ripple cross-laminated, light grey very fine- to fine-grained sandstone forming amalgamated units up to 2.20 m thick. Internal second-order erosion surfaces separate hummocky cross-stratified laminasets. Locally, discrete hummocky and cross-laminated beds are separated by thin mudstone partings. Hummocky cross-stratification includes both isotropic and anisotropic types. Climbing ripples are symmetrical to quasi-symmetrical. Soft-sediment deformation structures, including load casts, pseudonodules, balls-and-pillows and convolute lamination, are common. Wood and plant fragments occur on some bedding planes	*Skolithos linearis*	Combined wave surges and unidirectional currents above fair-weather wave base	Distal delta front of a mixed wave- and river-influenced delta
	Facies B3: En echelon, trough cross-bedded and horizontally bedded medium- to fine-grained sandstone	En echelon bedsets of medium- to fine-grained sandstone (seaward-dipping clinoforms) locally overlain by erosive-based, lenticular trough cross-stratified medium- to fine-grained sandstone and horizontally bedded medium-grained sandstone (topsets) forming amalgamated intervals up to 50 m thick	None	Mouth-bar progradation and subsequent scouring	Proximal delta front and terminal distributary channels of a mixed wave- and river-influenced delta

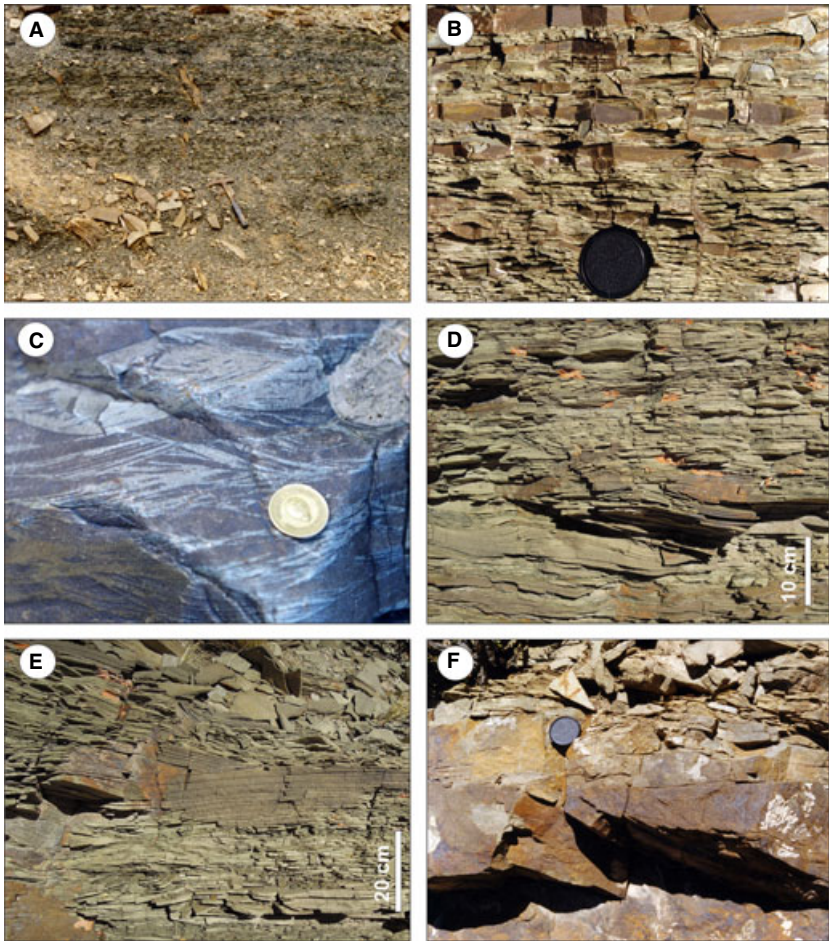

Fig. 3 Facies association A (Wave-dominated shallow marine). Lower interval of the Jarillal Member succession. (A) Facies A2, lower-offshore deposits characterized by siltstone units intercalated with thin very fine-grained sandstone beds. Hammer is 33 cm long. (B) Facies A3, upper-offshore deposits showing a regular intercalation of siltstone and very fine-grained sandstone with wave- and combined-flow ripple cross-lamination. Lens cap is 5.5 cm wide. (C) Facies A3, upper-offshore deposits. Close-up of wave-ripple cross-lamination displaying characteristic chevron upbuilding. Coin diameter is 1.8 cm. (D) Facies A4, offshore-transition deposits. Note hummocky beds passing upwards into a zone with combined-flow ripple cross-lamination and/or symmetrical to quasi-symmetrical ripples. Anisotropic hummocky is indicated by preferred dip direction of cross-strata sets. (E) Facies A5, lower/middle-shoreface deposits characterized by amalgamated hummocky cross-stratified very fine-grained sandstone. (F) Facies A6, upper-shoreface deposits showing planar cross-stratified medium-grained sandstone. Lens cap is 5.5 cm wide.

former consists of six facies (A1–A6), encompassing shelf, lower-offshore (Fig. 3A), upper-offshore (Fig. 3B-C), offshore-transition (Fig. 3D), lower/middle-shoreface (Fig. 3E) and upper-shoreface (Fig. 3F) deposits. This facies association is present in the lower and middle interval of the Jarillal Member, and deposits are stacked forming several coarsening-upward parasequences. In the lower interval, parasequences are sand-rich and tend to be dominated by proximal facies (Fig. 2). These lower parasequences are stacked forming a progradational parasequence set, reflecting an overall regressive trend. In the middle interval, parasequences are mud-rich and tend to be dominated by distal facies (Fig. 2). The middle interval records a transgression along a wave-dominated shoreline. Wave dominance is indicated by the abundance of structures indicative of oscillatory flows (Fig. 3B-E), including hummocky cross-stratification, and combined-flow and wave ripples, displaying diagnostic features such as chevron and bundled upbuilding and offshooting.

Facies association B consists of three facies (B1–B3), including various subenvironments of a prograding mixed wave- and river-influenced delta, such as prodelta (Fig. 4A), distal (Fig. 4B) and proximal delta front (Fig. 4C,E), and terminal distributary channels (Fig. 4D). This facies association is present in the upper interval of the Jarillal Member. The upper interval consists of coarsening-upward parasequences stacked forming a progradational parasequence set (Fig. 2). Deltaic progradation is further indicated by the presence of seaward-dipping clinoforms and delta topsets. Intense soft-sediment deformation (Fig. 4B) suggests high sedimentation rates and unstable substrate conditions, which is consistent with a deltaic setting.

MATGROUND FACIES

Microbially induced sedimentary structures (MISS) result from interaction between mat-forming microorganisms and sediment particles (Noffke, 2010 and references therein). In the studied succession, abundant MISS occur at eleven surfaces within a resistant cliff-forming sandstone unit that marks the top of the middle interval (Fig. 5A-C). These structures occur in hummocky cross-stratified to wave-rippled cross-laminated very fine-grained sandstone forming lower- to middle-shoreface deposits. Some of the bedding

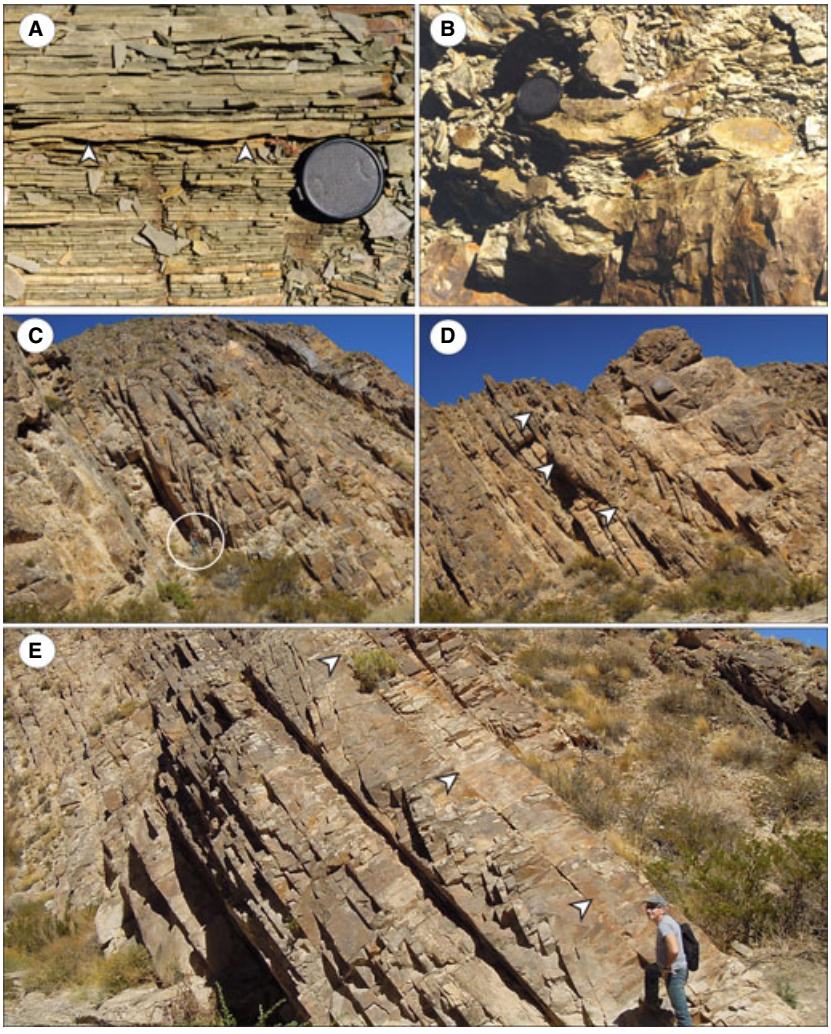

Fig. 4 Facies association B (Mixed wave-and river-influenced delta). Upper interval of the Jarillal Member succession. (A) Facies B1, prodelta deposits. Note dominance of thinly interbedded siltstone and sandstone and intercalation of a tabular, combined-flow ripple cross-laminated sandstone bed (arrow). Lens cap is 5.5 cm wide. (B) Facies B2, distal delta-front deposits, showing intense soft-sediment deformation. Lens cap is 5.5 cm wide. (C) Facies B3, proximal delta-front deposits forming seaward-dipping clinoforms. Geologist for scale (circled). (D) Facies B3, proximal delta-front deposits. Note clinoforms and terminal distributary-channel deposits forming an erosive-based lenticular sandstone body (arrow). (E) Facies B3, proximal delta-front deposits. Note seaward-dipping clinoforms and horizontally bedded topsets (arrow). Geologist for scale.

planes containing MISS can be followed laterally for approximately 500 m (Fig. 5A).

Manchuriophycus

The most pervasive MISS in these deposits are cracks referred to as 'Manchuriophycus' (Endo, 1933). These cracks are commonly preserved on the soles of sandstones and seem to be preferentially developed in the troughs of flat-topped ripples forming sinuous, curving positive patterns that cross-cut each other (Fig. 6A-D, Fig. 7A-B). In some cases, these structures are also preserved as negative features at the bases of the rippled sandstones. Cracks are 0.1–1.0 cm wide, and several centimetres long. These structures have been observed on nine different surfaces in the middle interval. Schieber (2004) considered these cracks as formed by destruction processes, such as dehydration and shrinkage. Most likely these cracks formed preferentially along the ripple troughs due to the presence of thicker microbial mats in those areas than in the crests (Schieber, 2007; Eriksson *et al.*, 2007; Lan & Chen, 2012). Thin sections revealed the presence of thick microbial mats that form a continuous layer draping the sediment surface (Fig. 6D). Some oriented sand grains are also visible within the organic matrix, mostly in areas with thicker epibenthic microbial mats. Haematite crystals are common, most likely representing weathered products of pyrite (Noffke *et al.*, 2006). Manchuriophycus has been reported in coastal areas of shallow-marine and lacustrine environments (Eriksson *et al.*, 2007; Schieber *et al.*, 2007). The co-occurrence of sinuous cracks with wave-ripple marks points to a subaqueous origin for these cracks (Lan & Chen, 2012).

Multidirected ripple marks and load-casted ripples

The other abundant MISS are multidirected ripple marks, which consist of patches of ripples having different orientations, preserved on the same surface. These structures are present on both the tops and bases of the sandstone beds, in the latter case forming load-casted ripples (Fig. 8A-D).

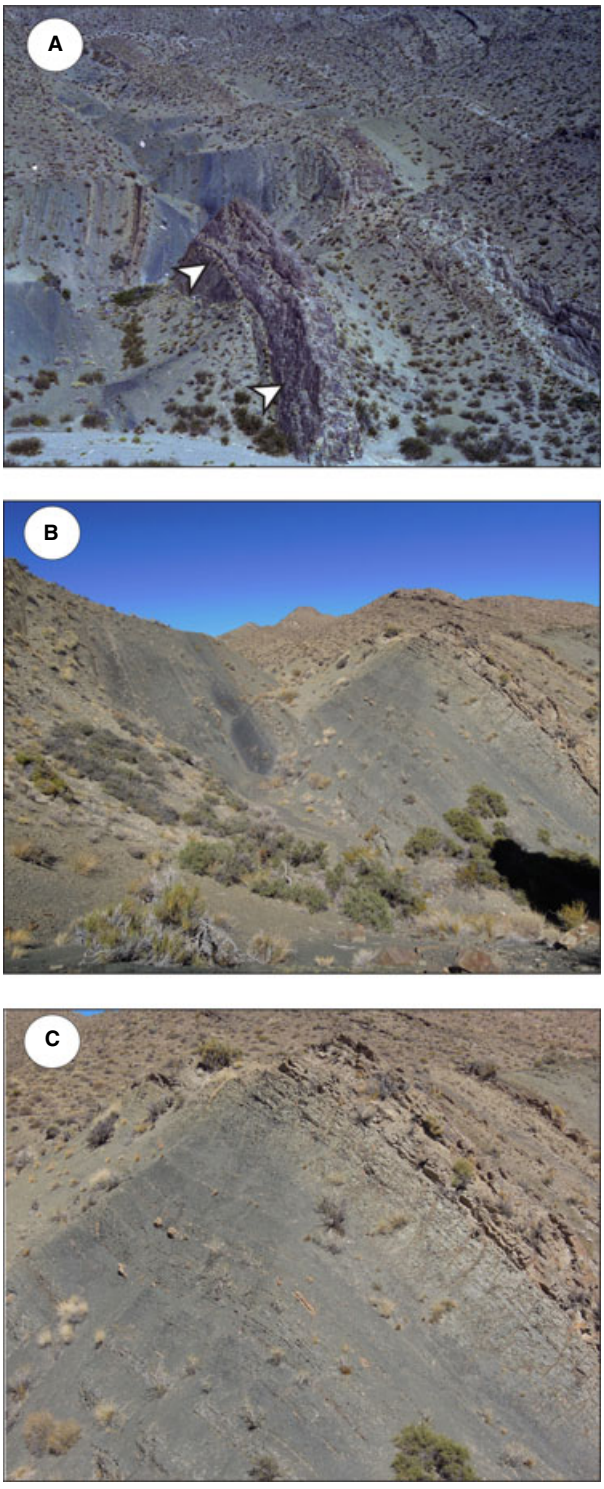

Fig. 5 Stratigraphic context of the matground facies occurrence in the middle interval of the Jarillal Member succession. (A) General view of the transgressive mudstone-dominated deposits of the middle interval. Arrow indicates location of MISS interval at the top of a wave-dominated parasequence. (B) General view of parasequence culminating in the lower/middle-shoreface deposits containing the MISS on the right. Note maximum-flooding shelf black shales on the left (Facies A1). (C) Close-up of the parasequence containing the MISS interval.

Multidirected ripple marks occur in at least eight closely spaced surfaces within the uppermost sandstone unit of the middle interval. These structures reflect the periodic alternation between mat growth, biostabilization and reworking by storms or high water during spring tides in shallow-water settings (Noffke, 1998; Pflüger, 1999; Draganits & Noffke, 2004; Bottjer & Hagadorn, 2007). Load-casted ripples record the moulding and exquisite preservation of bedforms in the absence of erosion due to microbial stabilization. Their occurrence suggests the presence of slimy films that provided cohesiveness to the deformed sandy beds, which were subsequently casted by a finer-grained bed (Seilacher, 2008; Bottjer & Hagadorn, 2007). These structures commonly are associated with palimpsest ripples in intertidal marine environments (Bottjer & Hagadorn, 2007), although in the Jarillal Member they are present in shoreface (i.e. below the low tide line) deposits.

DISCUSSION

As a result of the Cambrian Agronomic Revolution, microbial mats experienced a retreat towards environments hostile to bioturbators, essentially disappearing from fully marine settings by the Ordovician (Seilacher & Pflüger, 1994; Seilacher, 1999; Hagadorn & Bottjer, 1999; Buatois & Mángano, 2011a,b). Therefore, post-early Palaeozoic marine recordings of microbial mats are typically restricted to marginal-marine intertidal settings or fully marine settings under dysoxic conditions. Examples of the former are known from a number of tidal-flat deposits of Carboniferous age in Kansas (e.g. Mángano *et al.*, 2002; Buatois & Mángano, 2011b), Cretaceous age in Colorado (Schieber, 2007) and Neogene age in Patagonia (Carmona *et al.*, 2012). Examples of matgrounds in fully marine dysoxic environments have been documented in the Silurian of Lybia (Pflüger, 1999). Extensive matgrounds in fully marine settings are also known to occur at a more global scale as a result of mass extinctions. Suppression of bioturbation during biotic crises has resulted in the brief re-appearance of matgrounds, as illustrated by post-extinction aftermath Lower Triassic deposits, which contain abundant MISS (Pruss *et al.*, 2004).

The presence of extensive matgrounds in Carboniferous-Permian open-marine deposits of the Santa Elena formation illustrates an occurrence of anachronistic facies. As is the case of older rocks (Mata & Bottjer, 2009), there is evidence of mutual exclusion of matgrounds and penetrative bioturbation in the Santa Elena Formation. While vertical bioturbation is common in the nearshore deposits of the lower progradational parasequence set, penetrative trace fossils are absent or extremely rare in identical facies containing MISS in the transgressive interval, further suggesting that bioturbation is most likely a key factor precluding matground development. Brachiopod shells, which are abundant in the offshore tempestites and shoreface deposits of the lower

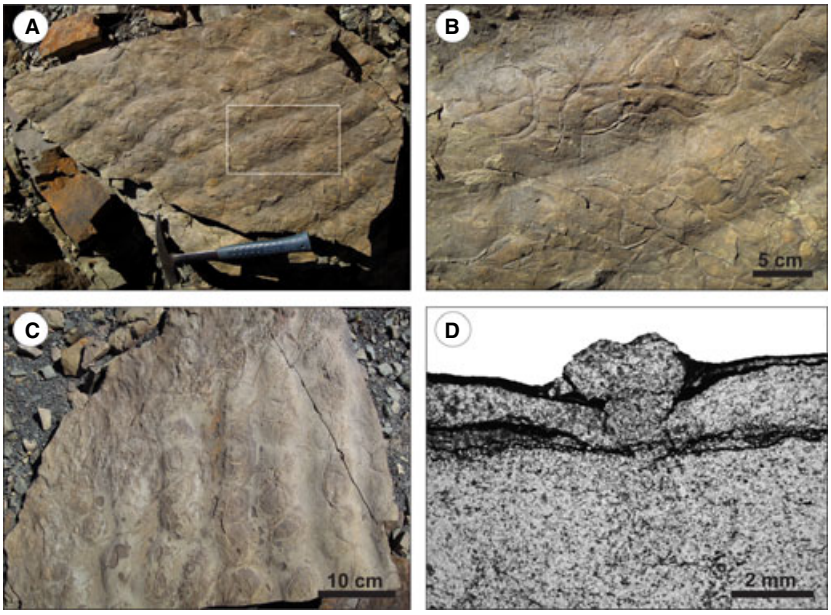

Fig. 6 Manchuriophycus. (A) General top view of microbially stabilized deposits showing flat-topped ripples and Manchuriophycus cracks. Hammer is 33 cm long. (B) Close-up view showing 8-shaped, circular and sinuous cracks. (C) Sandstone top with microbially induced shrinkage cracks. (D) Thin section, showing continuous microbial mats on the sediment surface, being disrupted by a shrinkage crack.

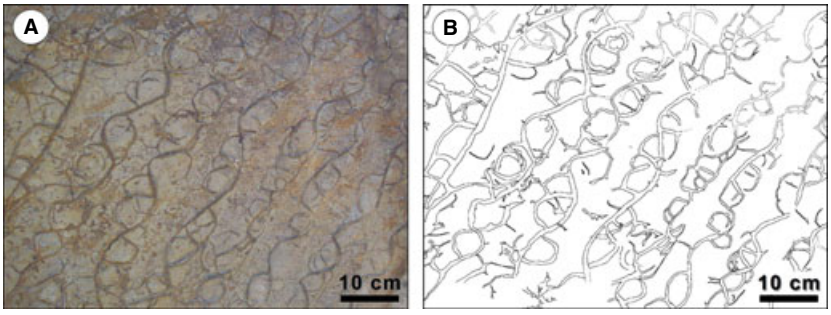

Fig. 7 Close-up of Manchuriophycus. Note the sinuous patterns and the superimposition of different crack generations. (A) Photograph. (B) Drawing.

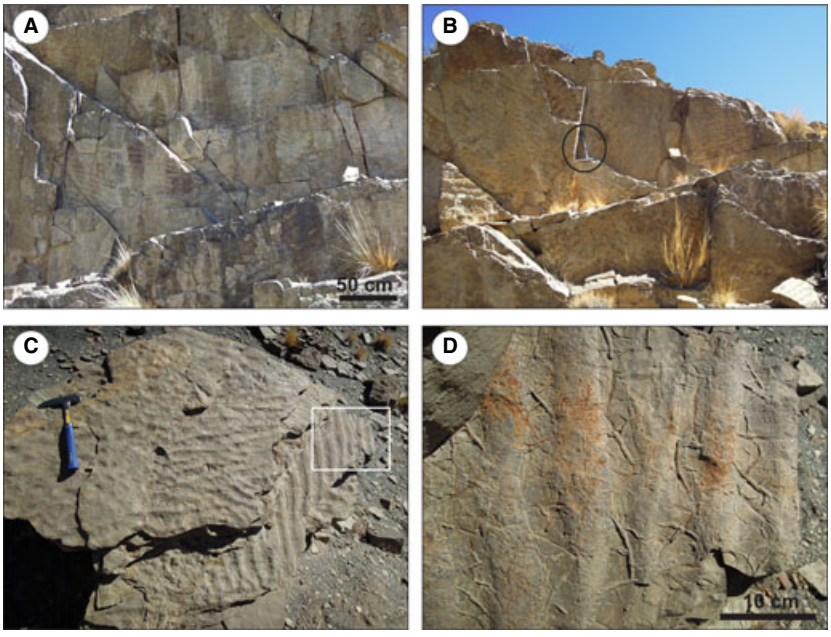

Fig. 8 Multidirected ripple marks and load-casted ripples. (A) General view of one of the sandstone bases showing load-casted ripples. (B) General view of sandstone tops with multidirected ripple marks and Manchuriophycus. Hammer (circled) is 33 cm long. (C) Different sandstone tops with multidirected ripple marks, flat-tops and cracks formed preferentially in ripple troughs. Hammer is 33 cm long. (D) Close up of C.

interval, are absent in the middle transgressive interval, further suggesting an environment hostile for the benthic fauna.

The occurrence of matgrounds in the Santa Elena Formation should be understood within the framework of the Gondwana glaciation. The Gondwana Ice Age comprises three main glacial events, namely Devonian-Early Carboniferous, early Late Carboniferous and Late Carboniferous-Early Permian (Limarino *et al.*, 2002). The second of these events is well represented in the Andean basins of Argentina, including the Calingasta-Uspallata Basin (López-Gamundí, 2010; Limarino *et al.*, 2002). However, it is the third event the one that records the peak of the Gondwana Ice Age, displaying the most widespread distribution of glacial deposits in eastern Argentina, Brazil, South Africa, Antarctica and Australia (López-Gamundí, 2010). Although glacial deposits of the Late Carboniferous-Early Permian event do not occur in the Andean basins, the deglaciation phase is indirectly recorded by a rapid rise in sea level resulting in a drastic landward facies shift forming a transgressive systems tract (Desjardins *et al.*, 2009; López-Gamundí, 2010). This Stephanian-Asselian transgression is evidenced in the Santa Elena Formation, as indicated by the thick mudstone-prone shelf deposits of the middle interval.

Extensive development of matground facies in deglacial times is not restricted to the Santa Elena Formation; MISS also occur in equivalent strata in southern Brazil (Rio do Sul/Taciba Formation, Paraná Basin). Palimpsest ripples, trapping and binding structures, erosional remnants, wrinkle structures, biolamination, sinoidal laminae and microbial filaments are common in the fine-grained rhythmites (Netto *et al.*, 2009). Bioturbation is absent and small-scale, soft-deformation structures are widespread. Framboidal pyrite and acritarchs occur locally.

Suppression of bioturbation may result from a number of stress factors, such as anoxia, episodic deposition, hypersalinity or extreme brackish-water (oligohaline) conditions (Buatois & Mángano, 2011a). In particular, changes of intensity of bioturbation and ichnodiversity occur along a salinity gradient within marginal-marine environments (Wightman *et al.*, 1987; Mángano & Buatois, 2004; Buatois & Mángano, 2011a; MacEachern & Gingras, 2007). Because very few animals have the physiological adaptations necessary to survive in brackish water, marginal-marine ichnofaunas are of low diversity. Ichnodiversity and degree of bioturbation are minimal under oligohaline conditions and may eventually fall to zero close to the transition to freshwater.

Isbell *et al.* (2003) estimated that the late Paleozoic Gondwana ice sheet volumes were in the range of 49.1–65.4 $\times$ 10^6 km^3. Full ablation of a single ice sheet would have resulted in a 100-m sea-level rise. Melting of the Gondwana ice masses may have caused an extreme discharge of freshwater (Buatois *et al.*, 2006, 2010), a situation somewhat comparable with that of the Holocene Yoldia Sea, which was freshwater during most of its deglaciation history as a consequence of the high release of meltwater in the northern Baltic Sea Basin (Virtasalo *et al.*, 2006). An unusual release of meltwater during the final deglaciation episode of the Gondwana Ice Age may have dramatically freshened peri-Gondwanan seas, impacting negatively on coastal and shallow-marine benthic faunas. Suppression of bioturbation was therefore conducive to a brief re-appearance of matground-dominated ecosystems.

The global impact of the Gondwana Ice Age and its transition to a largely ice-free greenhouse world on marine ecosystems have received increased attention through the documentation of low rates of origination and extinction during the glaciation and rapid faunal turnovers in its aftermath (e.g. Stanley & Powell, 2003; Clapham & James, 2008; Isbell *et al.*, 2008). On the other spectrum of the scale, the near-field effects (i.e. in close proximity to glaciers) of the deglaciation have been examined recently in the upper Paleozoic deposits of Gondwana with the documentation of freshwater ichnofaunas inhabiting coastal areas of fjord settings as a result of extreme meltwater release from adjacent ice masses (Buatois *et al.*, 2006, 2010). The present study bridges the gap between these two scales of analysis by showing that freshwater release was significant at a regional and inter-basin scale, with ablation of the Late Carboniferous-Early Permian ice cap affecting the Andean basins of Argentina. This is a scale that has received little attention in the stratigraphic record. However, information from modern environments shows that the impact of coastal processes far exceeds the local scale. For example, approximately 50% of sediment deposited in the Orinoco Delta is in fact derived not from the Orinoco River but from the mouth of the Amazon River, located some 2000 km to the southeast. The sediment is transported via the northwest-directed Guayana current, generating extensive muddy shorelines along the northern coast of South America (Kuehl *et al.*, 1986). Large-scale events, such as the deglaciation that immediately followed the Gondwana Ice Age, undoubtedly have played a major role on coastal ecosystems, strongly affecting benthic communities (Buatois *et al.*, 2006, 2010; Netto *et al.*, 2009, 2012). Bioturbation is a key factor in ecosystem performance which plays a major role in ocean and sediment geochemistry (e.g. Canfield & Farquhar, 2008). Accordingly, the decimation of the mixed layer (i.e. the soupy and totally bioturbated uppermost sediment zone) during deglaciation in the Gondwana basins may have altered ecosystem functioning and geochemical cycling. The geobiological consequences of the Gondwanan deglaciation event deserve further exploration.

ACKNOWLEDGMENTS

Financial support for this study was provided by Natural Sciences and Engineering Research Council (NSERC)

Discovery Grants 311727-05/08 and 311726-05/08, by The Brazilian Scientific and Technological Development Council (CNPq) Research Grants 305208/2010-1 and 401826/2010-4, and PI-UNRN 2011 40-A-158 and a Conicet (Argentinean Research Council) postdoctoral fellowship. Ana Archangelsky is thanked for calling our attention about the Uspallata structures, Oscar López Gamundí for his comments on the deltaic clinoforms of the Santa Elena Formation, and Pablo Gonzalez, Juan José Ponce and Constanza Bournod for valuable feedback on the thin sections. The Geobiology reviewers and editors Kurt Konhauser and Nick Butterfield provided very useful comments.

REFERENCES

Azcuy CL, Carrizo HA, Caminos R (1999) Carbonífero y Pérmico de las Sierras Pampeanas, Famatina, Precordillera, Cordillera Frontal y Bloque de San Rafael. In *Geología Argentina* (ed. Caminos R). Anales del Instituto de Geología y Recursos Minerales, Buenos Aires, **29**, PP. 261–318.

Bottjer DJ, Hagadorn JW (2007) Mat growth features. In *Atlas of Microbial Mat Features Preserved Within the Siliciclastic Rock Record* (eds Schieber J, Bose PK, Eriksson PG, Banerjee S, Sarkar S, Altermann W, Catuneanu O). Atlases in Geosciences. Elsevier, Amsterdam, pp. 53–71.

Buatois LA, Mángano MG (2011a) *Ichnology: Organism-Substrate Interactions in Space and Time*. Cambridge University Press, Cambridge.

Buatois LA, Mángano MG (2011b) The trace-fossil record of organism-matground interactions in space and time. In *Microbial Mats in Siliciclastic Sediments* (eds Noffke N, Chafetz H). Society for Sedimentary Geology Special Publication, Tulsa, **101**, pp. 15–28.

Buatois LA, Netto R, Mangano MG, Balistieri P (2006) Extreme freshwater release during the late Paleozoic Gondwana deglaciation and its impact on coastal ecosystems. *Geology* **34**, 1021–1024.

Buatois LA, Netto R, Mángano MG (2010) Ichnology of late Paleozoic post-glacial transgressive deposits in Gondwana: reconstructing salinity conditions in coastal ecosystems affected by strong meltwater discharge. In *Late Paleozoic Glacial Events and Postglacial Transgressions in Gondwana* (eds López-Gamundí OR, Buatois LA). Geological Society of America Special Paper, Boulder, **468**, pp. 149–173.

Canfield DE, Farquhar J (2008) Animal evolution, bioturbation, and the sulfate concentration of the oceans. *Proceedings of the National Academy of Sciences* **106**, 8123–8127.

Carmona NB, Ponce JJ, Wetzel A, Bournod CN, Cuadrado DG (2012) Microbially induced sedimentary structures in Neogene tidal flats from Argentina: paleoenvironmental, stratigraphic and taphonomic implications. *Palaeogeography, Palaeoclimatology, Palaeoecology* **35**, 3–355.

Clapham ME, James NP (2008) Paleoecology of early–middle Permian marine communities in Eastern Australia: response to global climate change in the aftermath of the late paleozoic ice age. *Palaios* **23**, 738–750.

Desjardins P, Buatois LA, Limarino CO, Cisterna G (2009) Latest Carboniferous-earliest Permian transgressive deposits in the Paganzo Basin of Western Argentina: lithofacies and sequence stratigraphy of a coastal plain to shallow-marine succession. *Journal of South American Earth Sciences* **28**, 40–53.

Dessanti RN, Rossi JJ (1950) Nuevos hallazgos de fósiles carboníferos en la Quebrada de Uspallata. *Revista de la Asociación Geológica Argentina* **5**, 149–158.

Draganits E, Noffke N (2004) Siliciclastic stromatolites and other microbially induced sedimentary structures in an early Devonian barrier-island environment (Muth Formation, NW Himalayas). *Journal of Sedimentary Research* **74**, 191–202.

Endo R (1933) Manchuriophycus, nov. gen., from a Sinian formation of South Manchuria. *Japan. Journal of Geology and Geography* **11**, 43–48.

Eriksson PG, Porada H, Banerjee S, Bouougri E, Sarkar S, Bumby AJ (2007) Mat-destruction features. In *Atlas of Microbial Mat Features Preserved Within the Siliciclastic Rock Record* (eds Schieber J, Bose PK, Eriksson PG, Banerjee S, Sarkar S, Altermann W, Catuneanu O). Atlases in Geosciences. Elsevier, Amsterdam, pp. 76–105.

Ezaki Y, Liu JB, Adachi N (2012) Lower Triassic stromatolites in Luodian County, Guizhou Province, South China: evidence for the protracted devastation of the marine environments. *Geobiology* **10**, 48–59.

Hagadorn JW, Bottjer DJ (1999) Restriction of a late Neoproterozoic biotope: suspect-microbial structures and trace fossils at the Vendian-Cambrian Transition. *Palaios* **14**, 73–85.

Isbell JL, Miller MF, Wolfe KL, Lenaker PA (2003) Timing of late Paleozoic glaciation in Gondwana: was glaciation responsible for the development of northern hemisphere cyclothems? In *Extreme Depositional Environments: Mega End Members in Geologic Time* (eds Chan MA, Archer AW) Geological Society of America Special Paper, Boulder, **370**, pp. 5–24.

Isbell JL, Fraiser ML, Henry LC (2008) Examining the Complexity of Environmental Change during the Late Paleozoic and Early Mesozoic. *Palaios* **23**, 267–269.

Kuehl SA, De Master DJ, Nittrouer CA (1986) Nature of sediment accumulation on the Amazon Continental Shelf. *Continental Shelf Research* **6**, 209–225.

Lan ZW, Chen ZQ (2012) Exceptionally preserved microbially induced sedimentary structures from the Ediacaran post-glacial successions in the Kimberley region, northwestern Australia. *Precambrian Research* **200-203**, 1–25.

Limarino CO, Césari SN, Net LI, Marenssi SA, Gutierrez RP, Tripaldi A (2002) The Upper Carboniferous postglacial transgression in the Paganzo and Rio Blanco basins (northwestern Argentina): facies and stratigraphic significance. *Journal of South American Earth Sciences* **15**, 445–460.

López-Gamundí OR (2010) Transgressions related to the demise of the late Paleozoic Ice Age: their sequence stratigraphic context. In *Late Paleozoic Glacial Events and Postglacial Transgressions in Gondwana* (eds López-Gamundí OR, Buatois LA). Geological Society of America Special Paper, Boulder, **468**, pp. 1–35.

MacEachern JA, Gingras M (2007) Recognition of brackish-water trace fossil assemblages in the Cretaceous western interior seaway of Alberta. In *Sediment-Organism Interactions: A Multifaceted Ichnology* (eds Bromley R, Buatois LA, Mángano MG, Genise J, Melchor R). Society for Sedimentary Geology Special Publication, Tulsa, **88**, pp. 149–194.

Mángano MG, Buatois LA (2004) Ichnology of Carboniferous tide-influenced environments and tidal flat variability in the North American Midcontinent. In *The Application of Ichnology to Palaeoenvironmental and Stratigraphic Analysis* (ed McIlroy D). Geological Society London Special Publication, London, **228**, pp. 157–178.

Mángano MG, Buatois LA, West RR, Maples CG (2002) Ichnology of an equatorial tidal flat: the Stull Shale Member at

Waverly, eastern Kansas. *Bulletin of the Kansas Geological Survey* **245**, 130.
Mata SA, Bottjer DJ (2009) The paleoenvironmental distribution of Phanerozoic wrinkle structures. *Earth Science Reviews* **96**, 181–195.
Mata SA, Bottjer DJ (2012) Microbes and mass extinctions: paleoenvironmental distribution of microbialites during times of biotic crisis. *Geobiology* **10**, 3–24.
Netto RG, Balistieri PRMN, Lavina EL, Silveira DM (2009) Ichnological signatures of shallow freshwater lakes in the glacial Itarare Group (Mafra Formation, Upper Carboniferous-Lower Permian of Parana Basin, S Brazil). *Palaeogeography, Palaeoclimatology, Palaeoecology* **272**, 240–255.
Netto RG, Benner JS, Buatois LA, Uchman A, Mángano MG, Ridge JC, Kazakauskas V, Gaigalas A (2012) Glacial Environments. In *Trace Fossils as Indicators of Sedimentary Environments* (eds Knaust D, Bromley RG) Developments in Sedimentology, Elsevier, Amsterdam, **64**, 297–336.
Noffke N (1998) Multidirected ripple marks rising from biological and sedimentological processes in modern lower supratidal deposits (Mellum Island, southern North Sea). *Geology* **26**, 879–882.
Noffke N (2010) *Geobiology: Microbial Mats in Sandy Deposits from the Archaean Era to Today*. Springer-Verlag, Berlin, Heidelberg.
Noffke N, Gerdes G, Klenke T, Krumbein WE (2001) Microbially induced sedimentary structures: a new category within the classification of primary sedimentary structures. *Journal of Sedimentary Research* **71**, 649–656.
Noffke N, Eriksson K, Hazen R, Simpson E (2006) A new window into Early Archean life: microbial mats in Earth's oldest siliciclastic tidal deposits (3.2 Ga Moodies Group, South Africa). *Geology* **34**, 253–256.
Pflüger F (1999) Matground structures and Redox facies. *Palaios*, **14**, 25–39.
Pruss S, Fraiser M, Bottjer DJ (2004) Proliferation of Early Triassic wrinkle structures: implications for environmental stress following the end-Permian mass extinction. *Geology* **32**, 461–464.
Schieber J (2004) Microbial mats in the siliciclastic rock record: a summary of diagnostic features. In *The Precambrian Earth: Tempos and Events, Developments in Precambrian Geology* (eds Eriksson PG, Altermann W, Nelson D, Mueller WU, Catuneanu O, Strand K). Elsevier, Amsterdam, pp. 663–672.
Schieber J (2007) Ripple patches in the Cretaceous Dakota Sandstone near Denver, Colorado, a classic locality for microbially bound tidal sand flats. In *Atlas of Microbial Mat Features Preserved Within the Siliciclastic Rock Record* (eds Schieber J, Bose PK, Eriksson PG, Banerjee S, Sarkar S, Altermann W, Catuneanu O). Atlases in Geosciences. Elsevier, Amsterdam, pp. 222–225.
Schieber J, Bose PK, Eriksson PG, Sarkar S (2007) Paleogeography of microbial mats in terrigenous clastics - environmental distribution of associated sedimentary features and the role of geologic time. In *Atlas of Microbial Mat Features Preserved within the Clastic Rock Record* (eds Schieber J, Bose PK, Eriksson PG, Banerjee S, Sarkar S, Altermann W, Catuneanu O). Elsevier, Amsterdam, pp. 267–275.
Seilacher A (1999) Biomat-related lifestyles in the Precambrian. *Palaios* **14**, 86–93.
Seilacher A (2008) *Fossil Art. An exhibition of the Geologisches Institut*, Tuebingen University, Tuebingen.
Seilacher A, Pflüger F (1994) From biomats to benthic agriculture: a biohistoric revolution. In *Biostabilization of sediments* (eds Paterson DM, Stal LJ, Krumbein WE). Bibliotheks und Informationssystem der Carl von Ossietzky Universität Odenburg, Odenburg, pp. 97–105.
Stanley SM, Powell MG (2003) Depressed rates of origination and extinction during the late Paleozoic ice age: a new state for the global marine ecosystem. *Geology* **31**, 877–880.
Taboada AC (1998) Dos nuevas especies de Linoproductidae (Brachiopoda) y algunas consideraciones sobre el Neopaleozoico sedimentario en las cercanías de Uspallata, Argentina. *Acta Geológica Lilloana* **18**, 69–80.
Taboada AC (1999) Bioestratigrafía del Carbonífero marino del Valle de Calingasta-Uspallata, provincias de San Juan y Mendoza. *Ameghiniana* **34**, 215–246.
Virtasalo JJ, Kotilainen AT, Gingras MK (2006) Trace fossils as indicators of environmental change in Holocene sediments of the Archipelago Sea, northern Baltic Sea. *Palaeogeography, Palaeoclimatology, Palaeoecology* **240**, 453–467.
Wightman DM, Pemberton SG, Singh C (1987) Depositional modelling of the Upper Mannville (Lower Cretaceous), east-central Alberta: implications for the recognition of brackish water deposits. In *Reservoir Sedimentology* (eds Tillman RW, Weber KJ). Society for Sedimentary Geology Special Publication, Tulsa, **40**, pp. 189–220.